



BOREHOLE GEOLOGY OF WELL SJ9-2, SAN JACINTO – TIZATE GEOTHERMAL FIELD, NW-NICARAGUA

Robertha Maria Quintero Roman

Ministry of Energy and Mines

Geothermal Direction

Managua

NICARAGUA

robertha.quintero@mem.gob.ni

ABSTRACT

Well SJ9-2 is located in the San Jacinto - Tizate high-temperature field in NW-Nicaragua. It is a directional well reaching a total depth of 1388 m with a sidetrack to 1725 m. The uppermost 1000 m were analysed through cuttings and thin sections; below 1000 m the analyses were based on thin sections. The lithology of well SJ9-2 comprises a volcanoclastic sequence which consists of tuff with intercalated andesite and basaltic andesite; three different types of tuff formations have been distinguished based on texture, crystallinity and compositional variation. Hydrothermal alteration is controlled by temperature, rock type and permeability. The mineral assemblage showed that the alteration temperature increased with depth, first with the appearance of minerals such as low-temperature zeolites, quartz, and smectite. The alteration reflects higher temperatures below 519 m depth with the appearance of epidote (sparse) and wairakite ($\geq 230^{\circ}\text{C}$). The alteration increased below 900 m depth (epidote abundant, $\geq 250^{\circ}\text{C}$) and localized at 1250-1350 m depth (actinolite, $\geq 280^{\circ}\text{C}$). Four alteration zones were identified in the well: an argillic zone at 12-303 m, phyllic alteration at 303-519 m, a propylitic zone at 519-1281 m and a high-temperature propylitic zone at 1281-1329 m. The propylitic zone reappears at 1329-1725 m depth. The permeability in the well is negligible. According to the circulation losses and temperature profile, six small aquifers were identified in the production zone. Comparison of alteration mineral temperature and measured temperature showed that the geothermal system is overall in equilibrium with a reservoir temperature of 240-255°C.

1. INTRODUCTION

Nicaragua is a country with great geothermal potential due to the presence of the volcanic mountain chain Maribios that runs parallel to the Pacific Coast. The Maribios volcanic chain consists of active volcanoes, some lagoons, volcanic structures, and extensive areas of hydrothermal activity denoting the presence of a magmatic heat source at depth. Many geoscientific studies have been performed since 1966 by various institutions in the country through recruitment of foreign consulting firms with the aim of evaluating the geothermal potential of Nicaragua (CNE, 2001). The development of the geothermal resources in Nicaragua would contribute to changing the current energy situation in the country.

The Nicaraguan Government has made efforts to promote investments in electricity generation from renewable resources, which can be implemented by private companies, by the state or both. One of the main priorities of the Nicaraguan state is the urgency of changing the energy matrix since the recent increase in the price of fossil fuel has significantly increased the cost of electricity, affecting the country's economic stability.

The high geothermal potential in Nicaragua is an opportunity for the nation to meet a significant part of its energy demand by using this clean renewable resource. By developing geothermal energy, Nicaragua could gradually achieve a significant change in the energy matrix while simultaneously reducing the environmental impact from power generation, as geothermal energy is a relatively low carbon dioxide emitting source of energy. A successful development of geothermal energy would, therefore, contribute significantly to reducing greenhouse gas emissions that contribute to climate change on our planet. Geothermal power is also a good base load energy resource with a load factor of up to 95%, which is independent of climatic factors.

Since the publication of the Master Plan (CNE, 2001), four geothermal concessions have been awarded in Nicaragua to private foreign companies: San Jacinto - Tizate which is in exploitation stage, and Hoyo - Monte Galan, Managua - Chiltepe, and Casita - San Cristobal, which are still in the exploration stage; two exploration wells have been drilled in Hoyo - Monte Galan and Managua - Chiltepe.

1.1 Development of the San Jacinto - Tizate geothermal area

The San Jacinto - Tizate geothermal field is located in the north-western part of the Nicaraguan depression, in the western part of Nicaragua (20 km south of Leon city). In 2001, San Jacinto - Tizate Power Company was awarded an exploitation licence for the San Jacinto - Tizate concession. This was later transferred to the Canadian company Polaris Energy. In August 2008, phase I of drilling was completed including three production wells and one reinjection well. The outcome was positive with one 16 MWe well. Phase II is currently under development during which Polaris intends to drill a number of wells to supply the necessary amount of steam for a second 36 MWe turbine.

1.2 Regional geology and tectonic setting of Nicaragua

Nicaragua is located in the centre of the Chortis block, which is a unit of the continental crust that belongs to the Caribbean plate (Figure 1). The subduction of the Cocos plate beneath the Caribbean plate has resulted in the formation of an active volcanic arc with a NW-SE orientation known as the Cordillera de Los Maribios within the Nicaraguan depression, parallel to the Pacific coast and the Mesoamerican trench. Numerous volcanoes make Nicaragua the country with the highest geothermal potential in Central America.

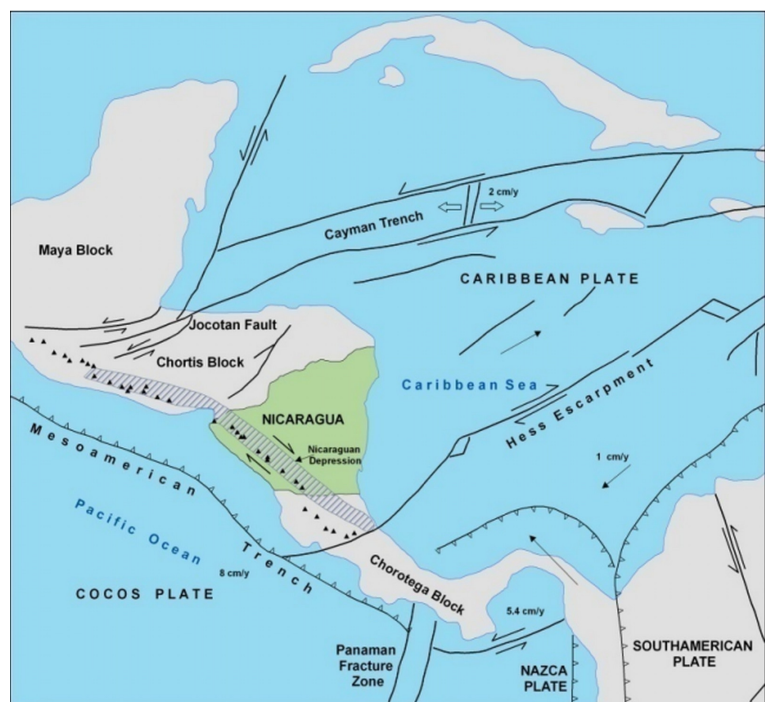


FIGURE 1: Tectonic scheme of Central America (CNE, 2001)

The chain of 18 distinct volcanic centres found in Nicaragua is a part of the Central America Volcanic Arc (CAVA) which extends along the Pacific coastline of the Central American Isthmus, from Guatemala in the northwest through Belize, El Salvador, Honduras, Nicaragua, and Costa Rica to Panama in the southeast (CNE, 2001), as seen in Figure 2. The Nicaraguan depression is one of the tectonic structures that can be found in the marginal Pacific zone of Central America, extending across Nicaragua from the Fonseca Gulf to the coast of Costa Rica. The depression is partially occupied by Lake Managua and includes the volcanic chain that extends NW-SE from the volcano Cosiguina to the Maderas volcano (Figure 2).



FIGURE 2: The volcanic chain of Nicaragua (MEM, 2008)

Weinberg (1992) identified three different phases of deformation that accompanied the geological evolution of the Pacific region of Nicaragua: 1) Miocene phase, 2) Pliocene-Lower Pleistocene phase and 3) Upper Pleistocene-Holocene phase. During the Miocene to Pliocene-Lower Pleistocene phase, the tectonic regime was dominated by a NE-SW orientated compression, normal to the Mesoamerican trench. During the Pliocene-Lower Pleistocene, the angle of subduction of the Cocos Plate is thought to have increased, reducing the speed of convergence of the Cocos and Caribbean Plates. From the upper Pleistocene-Holocene, a new regime began where tectonic stress was characterised by lateral strike-slip faulting and normal faults, and pull-apart structures were more evident; this became known as the Managua Graben. This resulted in a migration of volcanism westward towards the Pacific. The

deformation was mainly accommodated through normal faults, such as those that led to the development of the Nicaraguan Depression (Weinberg, 1992).

McBirney and Williams (1965) describe the geology of the volcanic chain in Nicaragua. The stratigraphy is divided into sequences of neritic sediments, mostly volcanoclastic, that were deposited between the late Cretaceous and upper Miocene. Formations from this interval include the Brito, Rivas, Masachapa and El Fraile formations. These formations are folded, eroded and covered by carbonate rocks and clastic sediments of the Pliocene (El Salto formations) and of volcanic rocks of the Las Sierras formation. In the NW sector of the Pacific coast are outcrops with thin layers of ignimbrites and lavas known as the Tamarindo group which is very similar to the El Fraile formation.

The interior plateau consists of volcanic rocks of the Matagalpa group (Oligocene) and Coyol group (Mio-Pliocene), which are composed of pyroclastic flows, ignimbrites, lavas of different composition and volcano-sedimentary rocks.

2. LOCAL GEOLOGY

2.1 San Jacinto – Tizate geothermal field

The San Jacinto – Tizate geothermal field is located in the northwest part of Nicaragua in the Marrabios volcanic chain, about 90 km from Managua, 10 km northeast of Telica and 20 km south of Leon. The San Jacinto – Tizate field constitutes the base of the eastern flank of the Telica volcanic massif (Figure 3).

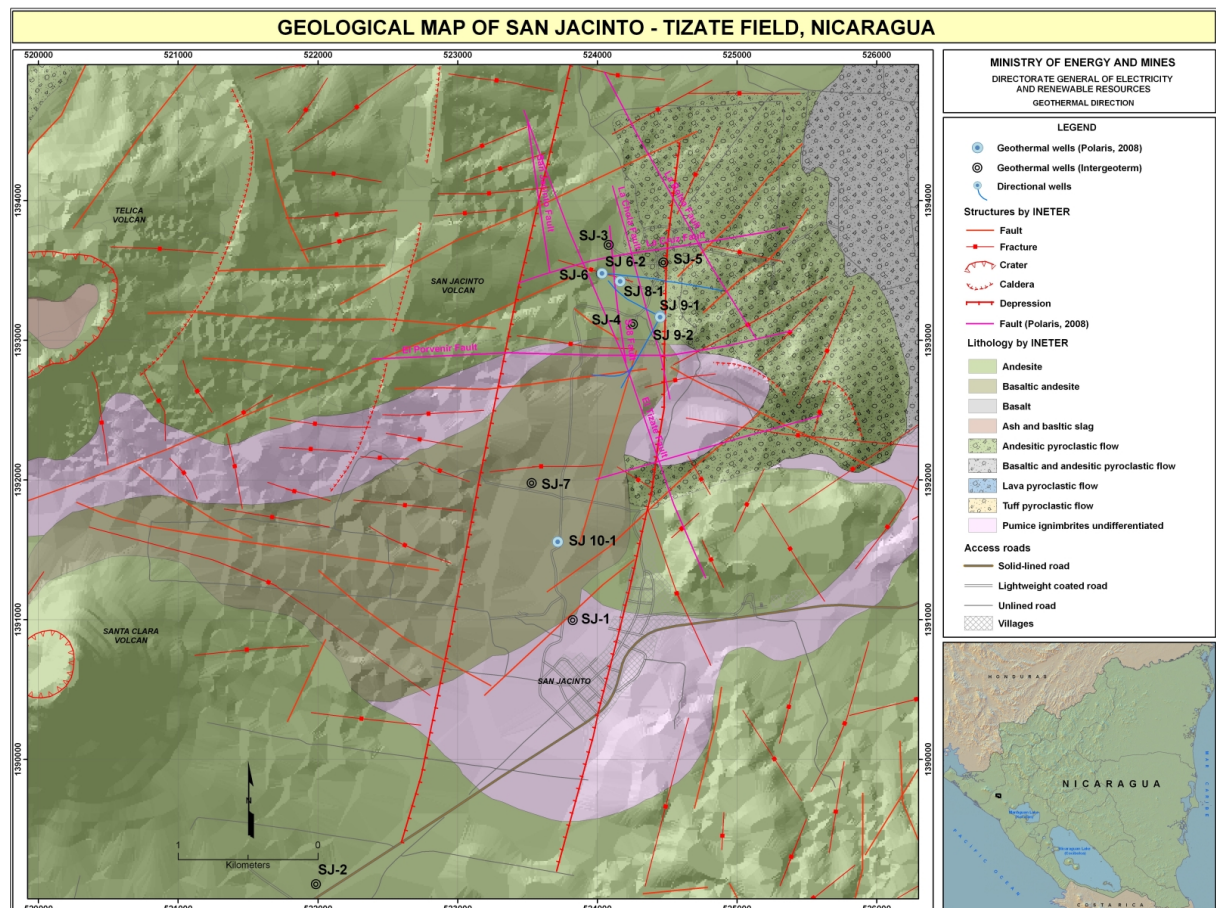


FIGURE 3: Geological map of San Jacinto - Tizate (MEM, 2008)

The eastern slope of the Telica volcanic massif includes the lower slopes of San Jacinto volcano, Santa Clara volcano and the reliefs of the old volcanic edifice El Chorro. The Rota volcano is located to the south. On the plains east of San Jacinto-Tizate are two small lava domes (Lomas de San Ignacio del Bosque) which are associated with craters produced by phreatic explosions (Lomas de Apante) and an extensive basaltic lava flow (La Campana - Valle Las Zapatas) (CNE, 2001).

Telica forms the westernmost part of a ridge running east-west with an apparent increase in age towards the east. Santa Clara Volcano is located to the south of the eastern part of the ridge and is reported to have erupted during the 1600s. However, it is possible that the eruption could have been centred on Telica. The youngest volcanism northeast of El Tizate appears to be the Don Bosco Domes. They have a young appearance and lie nested within tuff cones. There is a third tuff cone to the east that lacks a central dome, and there are remnants of older ones to the northwest. Superficially, the domes appear younger than El Chorro (CNE, 2001) and are estimated at an age of 150,000 years. Activity in the various centres of the Telica volcanic complex has been mainly effusive, with rocks of variable composition between basaltic and andesitic (CNE, 2001).

2.2 History of development

In the period June 1969 to February 1971, the Government of Nicaragua initiated geothermal exploration, retaining the services of the U.S. company Texas Instruments, Inc., which conducted early research into the existence of geothermal fields in Nicaragua. This programme was funded by the Agency for International Development of the United States and was designed to locate the first geothermal areas in the country suitable for geothermal development. This study included geological mapping with special attention to areas with hydrothermal alteration, geochemical and geophysical exploration (geoelectric, magnetotelluric and gravity). As a result of this study, two priority areas were selected for development: San Jacinto – Tizate and Momotombo.

During the years 1993-1995, the company Intergeoterm SA (ENEL Consortium Nicaragua-Russian Business) drilled seven exploration wells in the geothermal area of San Jacinto – Tizate to depths between 550 and 2000 m, resulting in three producing wells and one reinjection well. The production tests demonstrated the commercial viability of the field with a proven capacity of 25 MW.

The San Jacinto-Tizate field was awarded under an operating agreement for a period of 25 years to the company Intergeoterm S.A. in January 2001. In 2004 this was transferred to San Jacinto Power Company S.A. which is operated by the Canadian company Polaris Energy Nicaragua S.A. (PENSA). Electricity production began in June 2005 with the commissioning of a power plant with an 8 MW backpressure unit using two production wells and two reinjection wells. In June 2007, a second phase of deep drilling was launched with the objective of expanding the capacity of the field to a total of 72 MW.

2.3 Lithostatigraphy of San Jacinto – Tizate

The geological succession of the field has been investigated to a depth of 2300 m through drilling. It consists mostly of igneous, pyroclastic and intrusive rocks of basic-to-intermediate composition and sedimentary deposits of primary volcanic origin. The age of the rocks varies from late Miocene to Holocene. Four different stratigraphic units were identified, including pyroclastic-effusive units of the recent San Jacinto, Santa Clara and Rota volcanoes, a late Pleistocene unit of the El Chorro-Tizate volcano, the extrusive domes of Ignacio del Bosque, proluvial sediments of the San Jacinto Depression, and other units encountered only in the deep wells (Spektor, 1994). Generally, the geological column of the San Jacinto-Tizate field can be subdivided into four main units (Ostapenko et al., 1998, Figure 4):

Unit 1: Holocene age (QIV): The unit is composed of deposits of Holocene volcanoes. It includes andesites, basalts and tuffs of similar composition, as well as proluvial sediments filling the San Jacinto Depression. The lower part of this ~200 m thick unit is strongly altered (argillitic zone).

Unit 2: Pleistocene age (QI-III): This unit is composed of andesitic and andesitic-basalts, with intercalations of tuffs. The upper part of the approximately 800 m thick unit is altered (argillitic zone).

Unit 3: Pliocene and early Miocene age (N) is composed of pyroclastic rocks and agglomeratic tuffs, with intercalations of andesites and basalts. The thickness of the unit is about 1000 m.

Unit 4: Late Miocene age (NI) is composed of pyroclastics and sedimentary rocks (sandstones, gritstones and graywackes) of primary volcanic origin with rare intercalations of andesites and basalts. In the San Jacinto area, a section of andesites and basalts was encountered at a depth of 1800-2300 m. The thickness of the unit exceeds 500 m.

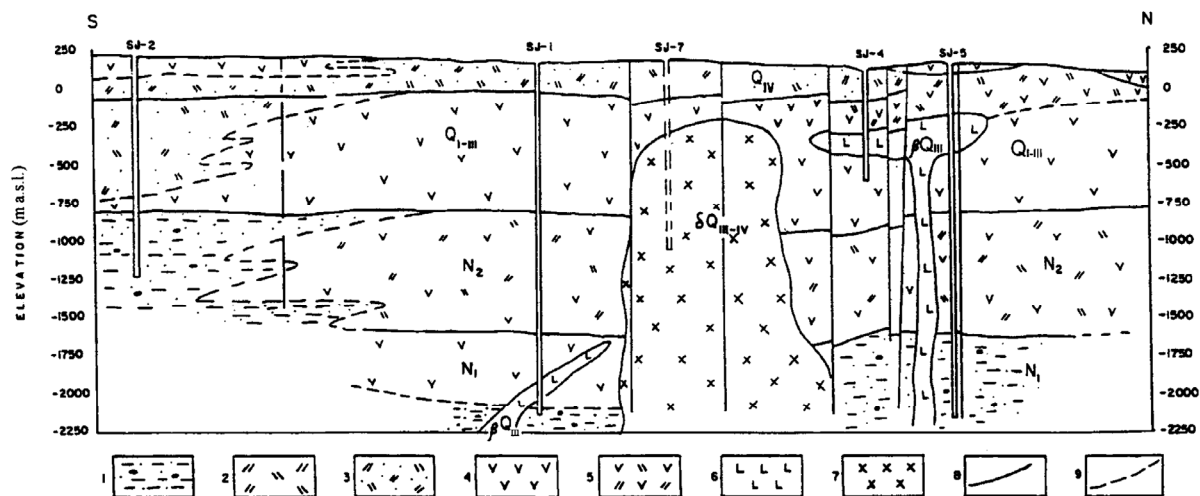


FIGURE 4: N-S geological cross-section of the San Jacinto-Tizate field: 1. Sedimentary rocks of volcanic origin; 2. Tuffs; 3. Intercalations of tuff and sedimentary rocks; 4. Andesite and andesite basaltic lavas; 5. Intercalations of lavas, tuffs and sedimentary rocks; 6. Basalt neck; 7. Diorite intrusion; 8. Stratigraphic contacts; 9. Lithological contacts (Ostapenko, 1998); the current well field is located in the northern part of the cross-section

2.4 Geological structures

Three main groups of faults have been identified in San Jacinto-Tizate geothermal field: NNE-trending, NW-trending, and volcano-tectonic ring faults (Ostapenko et al., 1998). The NNE-trending faults appear in the upper part of the geological section as a manifestation of one of the regional faults, transverse to the axis of the Los Maribios volcanic chain. They caused the formation of the San Jacinto graben. The group of NW-trending faults is part of the regional system of faults sub-parallel to the axis of the Los Marrabios volcanic chain. The volcano-tectonic ring faults are associated with the step immersion block-faulting of the large volcano-tectonic Telica Depression.

The San Jacinto-Tizate geothermal field is located within the composite structure formed by the superposition of the San Jacinto graben on the eastern part of the volcano-tectonic Telica Depression. The size of this composite structure is 5 km in a north-northeasterly direction and 1.5 km in a southwesterly direction. The occurrence of the Pleistocene-Miocene units, covered by recent volcanic sediments, is characterised by down-stepping blocks extending from the eastern to the western boundaries of the composite structure. The northern part of the structure (Tizate area) is intensely fractured by the intersection of faults with different trends (Ostapenko et al., 1998) and this is the current location of the well field.

3. BOREHOLE GEOLOGY

This report is based on the borehole geology in the upper 1725 m of well SJ9-2 in the San Jacinto-Tizate Field. The geological and hydrothermal alteration data was collected from cutting analyses using a binocular microscope (Olympus SZ12) and thin-section petrography. A total of approximately 575 samples of drill cuttings, starting at a depth of 12 m and reaching down to 1725 m depth, were collected at 3 m intervals. Analyses to identify subsurface formations in the upper 1000 m of the well were based on binocular and thin section analyses of the cuttings, but below 1000 m depth, the analyses were based on petrographic analyses. Other methods used were X-ray diffraction (XRD) analyses for identification of clay types along with the Linkam fluid inclusion stage; analyses were used to determine the temperature at which the inclusions formed in the crystals.

The aim of this study was to conduct an assessment of the lithostratigraphy and alteration mineralogy of well SJ9-2 in the San Jacinto-Tizate field, based on the analysis of cuttings and drilling data; some of the information was provided by Polaris Energy.

Well SJ9-2 was the third well drilled in an initial program of three production wells and two reinjection wells planned to increase the steam production and reinjection capacity for the first 24 MWe development phase of San Jacinto-Tizate geothermal field. The well was designed to intersect the El Porvenir, SJ8 and El Tizate faults. The location of well SJ9-2 is show in Figure 3.

This report is the result of a study done during a six month training course at the UNU Geothermal Training Programme in Iceland in 2010.

3.1 Analytical method

In this report, four main analytical techniques were used described here below:

Binocular microscope analysis: In binocular analysis of cutting samples, a fairly large portion of each sample is analysed to help define the type and relationship of the host rock and the alteration mineralogy. The analysis of the cuttings collected during drilling was done using an Olympus binocular microscope. In this report, the first 1000 m of cuttings from well SJ9-2 were analysed.

Petrographic microscope analysis: These studies were employed in order to construct the overall geological framework of the wells and, in conjunction with other analyses, document and characterize geothermal fluid flow paths. Thin sections were prepared for different representative rock types to find the degree of alteration in the wells. Studies of these samples provided data including: rock type and mineralogy, the relative amount of overall alteration (alteration intensity), relative concentration and mineralogy of veins and the presence of cavity fillings as a function of depth. In this report, 21 thin sections from 51 to 1659 m depth were prepared.

X-ray diffractometer analysis: A standard X-ray diffraction (XRD) analysis technique is concerned primarily with structural aspects of clay minerals and permits quantitative determination of clays. Twenty four samples of clays were selected for analysis occurring from 36 to 1567 m depth in the well.

Fluid inclusion analysis: Fluid inclusion studies were implemented to assist in separating different thermal events and, thus, in assembling the thermal history of the system. Fluid inclusions in minerals represent trapped portions of the liquids and gases from which the crystal grew. Microthermometric measurements were performed at two intervals in the well (519-570 and 912-921 m depth) using a Linkam THMSG-600 stage.

3.2 Drilling of well SJ9-2

Well SJ9-2 is the tenth well drilled in the San Jacinto – Tizate geothermal field. The well pad has the UTM coordinates: Easting - 524153.7, Northing - 1392655.4, and it is located next to well SJ9-1 (Figure 3). SJ9-2 was drilled by Perforadora Santa Bárbara S.A. with a Massarenti 6000 drill rig. The well was deviated to the southwest, initially at a bearing of 210°. The well was spudded on the 25th of November, 2007.

Well SJ9-2 is a large diameter deviated well; it was drilled from a 4.5 m deep cellar. The 36” conductor casing was cemented into a hand excavated hole in the cellar floor, and extended to 3 m below the cellar floor. The 20” casing was set at a depth of 134 m and the kick-off point was about 50 m below that. The well angle was gradually built up to approximately 35° with the 13^{3/8}” casing set at 578 m depth. The 12^{1/4}” production section was drilled to the planned completion depth of 1200 m MD but due to minimal permeability the well was extended to 1388 m MD. At that point there were no significant losses and no good permeability. Excessive drag on the drill string as well as limited output from the rig pumps (maximum 900 gpm) precluded drilling deeper. The hole was plugged with cement up to 900 m depth and it was decided to sidetrack the well to the west (bearing 260°).

The new leg was sidetracked in the 12^{1/4}” hole at 917 m and drilled to 1725 m depth. A 9^{1/2}” mud motor was used to build up inclination to a maximum of 40° to 955 m depth. The original 12^{1/4}” production hole was drilled from 583 to 1388 m using water. Due to limited capacity of the rig pumps and subsequent problems with well cleaning was the well drilled with a light mud from 955-1395 m depth. A 9 ^{5/8}” liner was installed at 775.3-1395 m depth before the well was completed to 1725 m depth with a 8^{3/4}” drill bit. The top of the liner 7” was set at 1301 m and the bottom of the liner at 1650 m (see Figure 5). Drilling of the sidetrack commenced on 10 December 2007, and the well was completed on 5 February 2008 (SKM, 2008a).

Partial circulation losses in SJ9-2 were encountered at 1157-1388 m, with an average rate of 20-25 bbl/h. In the sidetrack, losses of 60 bbl/h were recorded over the interval 1651-1714 m. However, this followed a period of hydrofracturing when the bit was at a depth of 1650-1651 m, during which maximum losses reached 850 bbl/h at a pressure of 1845 psi.

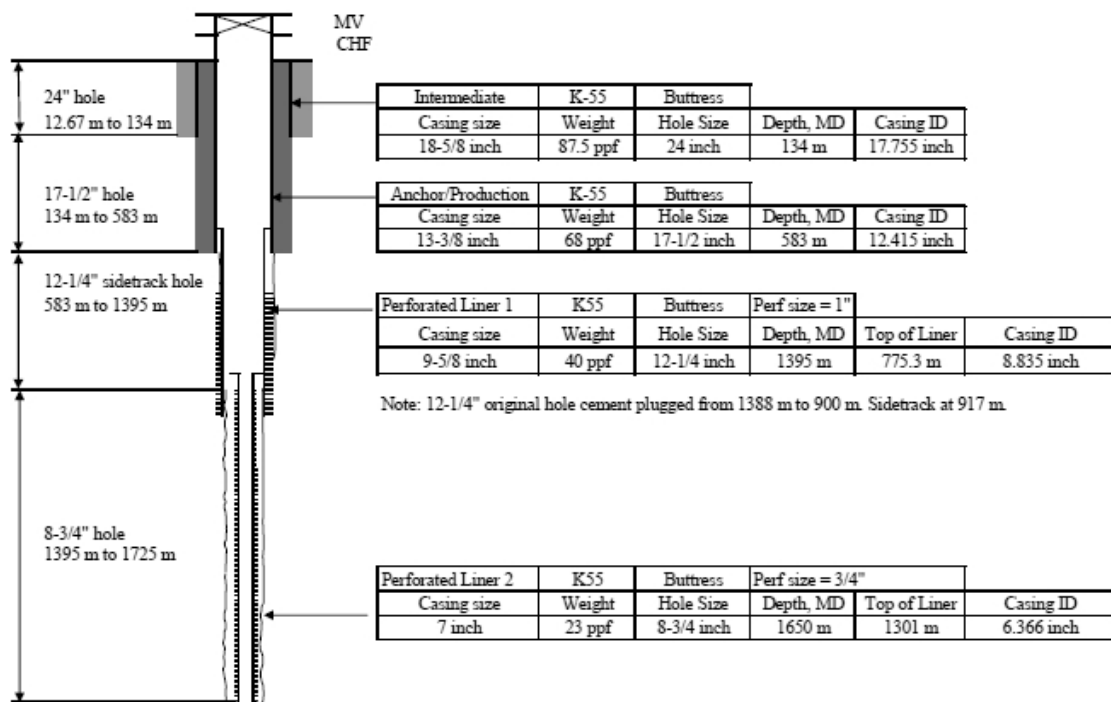


FIGURE 5: Casing programme of well SJ9-2 (SKM, 2008a)

3.3 Stratigraphy

The stratigraphy of well SJ9-2 from the surface down to 1725 m depth along the sidetrack is shown in Figure 6. A number of rock types were distinguished, based mainly on the crystallinity of the rocks. The stratigraphy in the well consists primarily of interlayered andesitic lavas and tuffs. The lava flows are classified as andesites, basaltic andesites or basalts, according to the texture and crystallinity of the rock and the presence of olivine, plagioclase and pyroxene (augite) phenocrysts in the samples. The tuffs were classified according to the proportion of glass, crystals and lithics in the rock as either vitric crystal tuff, lithic tuff or crystal lithic tuff. The description of the rock formation from well SJ9-2 in the first 1000 m is mainly based on binocular microscopic analysis with additional information from petrographic analysis, while the lower part of the well (below 1000 m) is based exclusively on petrographic analyses. The descriptions and characteristics of the unit are as follows:

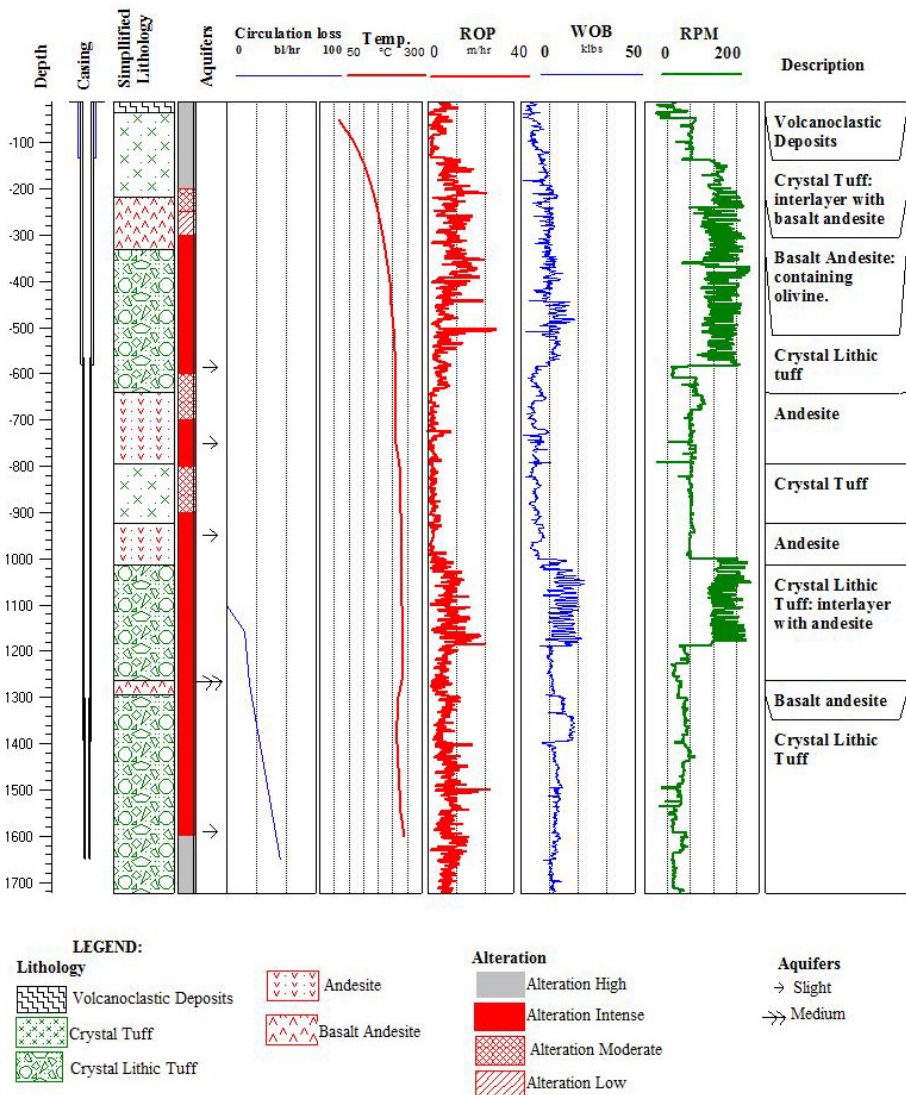


FIGURE 6: Simplified stratigraphic section in well SJ9-2

Volcanoclastic deposits (above-36 m): Sub- rounded to sub-angular brown fragments composed of pyroclastic material which is very highly altered. In thin section, kaolinite, smectite (confirmed with XRD analysis) and abundant calcite were observed.

Crystal tuff (36-219 m): A sequence of highly to intensely altered crystal tuff, which comprise subrounded lithics with phenocrysts of plagioclase and calcite in the groundmass. The tuff is vesicular, but most vesicles are filled by calcite or smectite (based in XRD); calcite vein fillings are present with disseminated pyrite. The crystal tuff is interlayered with thin lavas of basaltic andesite which are dark grey and have a porphyritic texture comprising pyroxene and plagioclase in the groundmass.

At 90-108 m depth there is a basaltic lava unit with sub-hedral plagioclase phenocrysts and altered olivine in the groundmass; the lava is intensely altered.

Smectite was observed at 99 m depth (thin sections) with low temperature zeolites (stilbite and heulandite). In cuttings, heulandite was observed at 117 m; at 129 m, rare small quartz crystals and rare chalcedony appeared. Veins were filled with calcite. At 201 m the composition of the rock changed and became more enriched in FeTi-oxides while the precipitation of calcite was pervasive.

Basaltic andesitic lavas (219-330 m): The basaltic andesitic lava sequence is dark grey in colour and with moderate alteration. The lavas have either an aphanitic texture or a porphyritic texture, comprised of euhedral plagioclase and pyroxene in a fine grained groundmass.

The alteration of the sequence is moderate except at 249-270 m depth, where the rock has a high grade of alteration. Calcite is generally found as fillings in vesicles as well as veins. Quartz vein fillings are also observed. Pyrite is disseminated in the rock. The content of green clay is moderate, but consists of interlayered clays (smectite and chlorite). According to petrographic observations, stilbite is still present and albite was observed replacing plagioclase.

Crystal lithic tuff (330-639 m): Pale green to white crystal lithic tuff. The tuff is fine-grained and crystalline with either small plagioclase phenocrysts or plagioclase glomerocrysts, while clinopyroxene phenocrysts are accessory. Thin units of glassy andesites are intercalated in the crystal lithic tuff.

The tuff is intensely altered into clay, but according to XRD analysis the clay consists of smectite and chlorite; the smectite content diminishes below 500 m depth.

Laumontite appears first at 393 m depth as small crystals and becomes more abundant with depth. Calcite is moderately abundant, but exhibits some variation in abundance with depth, while the content of pyrite is generally low in the sequence. Sparse epidote was identified at 600 m depth with petrographic analysis while wairakite was first identified at 561 m depth.

Andesitic lavas (639-795 m): Dark-grey, fine-grained andesite with plagioclase and pyroxene phenocrysts. At 654 m depth the andesite is more fine-grained and intensely altered. The interval with more intense alteration corresponds with the presence of calcite and pyrite vein fillings, while oxidation is less common. Within the sequences of andesitic lavas are interspersed with several thin units of crystal tuff. At 672 m depth the andesite is little altered and more dense and may represent an intrusion.

In the lower part of the sequence, below 711 m depth, alteration increases and, at the same time, laumontite and pyrite become more abundant. According to XRD analysis, chlorite is the prevailing type of clay below 650 m depth.

Crystal tuff (795-924 m): Pale greenish intensely altered crystal tuff with small plagioclase laths in the groundmass. With depth the crystal tuff becomes brownish in colour, where the alteration of the tuff is rather moderate. With depth the amount of epidote increases gradually. The first appearance of illite is identified with XRD analysis below 900 m depth. Laumontite is present as small, sparse crystals. Interstitial spaces are filled by calcite, chlorite and abundant pyrite.

Andesitic lava (924-1014 m): Pale grey to brownish andesitic lava sequence with euhedral pyroxene in a glassy groundmass. The lavas are moderately altered and mixed with minor amounts of crystal tuff. Quartz decreases in abundance with depth.

Crystal lithic tuff (1014-1263 m): Light-grey, fine-grained tuff, containing small crystals of plagioclase and pyroxene as well as sub-rounded lithic clasts within a consolidated groundmass. At 1218 m depth andesite lava fragments are abundant. The alteration is intense with abundant epidote from 1041 m depth. In some cases epidote has replaced plagioclase. The alteration mineral assemblage includes illite, chlorite, adularia, granular quartz, pyrite and abundant calcite and

wairakite. Prehnite appears at 1119 m depth.

Basaltic andesitic lavas (1263-1293 m): Porphyritic basalt with plagioclase (compositional range oligoclase-andesine), pyroxene and olivine phenocrysts. The basalt has a glassy groundmass. Trace amounts of tuff are observed in the sequence. The rock is intensely altered and actinolite has replaced olivine and pyroxene phenocrysts, while the plagioclase phenocrysts are replaced by albite. Alteration minerals are abundant, particularly wairakite, quartz and calcite; also primary minerals such as opaques (FeTi-oxides) are abundant. Chlorite is also identified, while illite is scarce.

Crystal lithic tuff (1293-1725 m): Pale grey crystal lithic tuff containing fine crystals of feldspar in the groundmass and many subrounded lithic fragments of predominantly dark grey andesite. The rock is very fine grained, while calcite and quartz are abundant.

In this part of the well the alteration is very strong, the oxidation is high and the plagioclase phenocrysts are replaced by calcite. Some vesicles are filled with clay and quartz, while the amount of epidote is decreasing. Chlorite and finely crystallized quartz are relatively common, while the content of illite increases.

4. HYDROTHERMAL ALTERATION

Hydrothermal alteration is the mineralogical, textural and chemical response of the rocks when subjected to drastic changes in their formation environment. The changes are influenced by permeability, temperature, pressure, rock types, fluid composition and duration of the activity (Browne, 1978). The essential feature of the hydrothermal alteration is the conversion of a set of initial minerals into a new association of more stable minerals. The original texture of the rock can be altered slightly or completely due to hydrothermal alteration.

The mineralogical alteration suites provide in-depth information on past and present characteristics of the geothermal system (Henley and Ellis, 1983). Hydrothermal alteration and mineralization are the results of an irreversible chemical exchange between an aqueous solution and adjacent rocks. Certain components are extracted selectively from the wall-rock and are added to the fluid and other components are selectively incorporated by the rocks and removed from the hydrothermal fluids. The result of this process depends on the physical conditions in the fluid-rock interface and on the relative amounts of fluid and rock involved in the chemical exchange process (water / rock interactions). Only the altered rock is the visible result of the process, because the fluid is removed from the system, except for possible fluid inclusions trapped in the precipitated minerals (Browne, 1978; Franzson, 2010). The secondary minerals form by different hydrothermal alteration processes (replacement, leaching (lixiviation) or deposition). The hydrothermal alteration processes cause chemical changes in the rock and the intensity of these varies with the mineralogy. In general terms the minerals more susceptible to alteration are (in order of decreasing susceptibility) olivine, magnetite, pyroxene, amphibole, mica, and feldspar.

The formation of selected alteration minerals is mainly dependent on temperature. Table 1 presents the temperature stability ranges of selected alteration minerals present in geothermal fields in Nicaragua (SKM, 2008b). Mapping the occurrence of alteration minerals with variable temperature stability ranges can then be used to correlate with the current formation temperature in the geothermal system and thus outline whether the system is in thermal equilibrium or whether heating or cooling has occurred.

The hydrothermal alteration produces different alteration mineral assemblages in the rock at progressively increasing temperatures in the geothermal system and is here classified into four alteration zones:

TABLE 1: Temperature at which selected alteration minerals occur

Minerals	T _{min} (°C)	T _{max} (°C)
Zeolites	30	130-150
Laumontite	120	190-220
Wairakite	200	
Smectite	50	< 200
MLC	200	230
Chlorite	230	≥300
Illite	230	≥300
Calcite	50-100	300
Quartz	160-180	≥300
Epidote	230-250	300
Actinolite	280	≥300

present along with calcite and pyrite. Propylitic alteration is commonly found at temperatures above 230-250°C.

The high-temperature propylitic alteration zone (sodium-calcium alteration zone) is characterised by the presence of actinolite in association with minerals such as albite, epidote, chlorite and quartz. High-temperature propylitic alteration usually occurs at temperatures above 280°C.

4.1 Primary rock minerals

The primary minerals in the rocks are unstable at high temperature and pressure, leading to their replacement by new minerals that are stable in the new formation environment (Browne, 1978). The primary minerals in the rocks penetrated by well SJ9-2 (Table 2) are characterised by an abundance of plagioclase, pyroxene, opaques (FeTi-oxides) and occasional olivine phenocrysts. The glass in the rock matrix is usually replaced by clay or calcite, more commonly seen in crystal tuff. The replacement of the minerals can be studied by petrographic thin section analysis.

TABLE 2: Alteration of the primary rock minerals found in well SJ9-2

Primary rock minerals	Alteration mineral products
Glass (matrix/tuff)	Clay, calcite, quartz
Olivine	Clay, quartz, actinolite
Plagioclase	Clay, albite, calcite, quartz, laumontite, wairakite, epidote
Pyroxene	Clay, actinolite, calcite
FeTi oxides	Titanite

Olivine is one of the primary minerals that forms basaltic rocks and is very susceptible to alteration. It occurs in sparse intervals along the extent of the well and was identified in a lithic tuff at 201m and 270 m depth where it was altered by clay, but it retains a prismatic shape. At 519 m depth, olivine appears to be replaced by quartz and clay, and at 1281 m depth olivine is replaced by actinolite.

Plagioclase is common and appears in the entire section of the well. From 12 to 99 m depth the plagioclase is strongly altered by kaolinite or replaced by albite. Below 100 m depth plagioclase has a subhedral to anhedral shape and is present as phenocrysts and as part of the groundmass. Fragments of the fresh and zoned plagioclase is observed in many intervals of the well, however the majority of the plagioclase is partially or completely altered by smectite, calcite, albite, zeolite, chlorite, and epidote.

The argillic alteration zone is characterised by the presence of smectite (montmorillonite) with substantial quantities of kaolinite or amorphous clays, mainly replacing plagioclase. There is significant leaching of Ca, Na and Mg from the rocks. Argillic alteration can develop in the temperature range of 50-200°C in the geothermal system.

The phyllic alteration zone is characterised by the presence of chlorite and/or illite. At phyllic alteration, feldspar (plagioclase and potassium feldspar) may be transformed to sericite and quartz, while the amount of kaolinite is minor. Phyllic alteration may represent a temperature range between 230-250°C.

The propylitic alteration zone is characterised by the presence of epidote, chlorite, illite and albite are also

Plagioclase in tuff showed more intense alteration than plagioclase in andesite, reflecting that the lavas unit in the well are more resistant to alteration than the tuffs. According to petrographic analysis, the types of plagioclase phenocrysts contained in the rocks are oligoclase and andesine below 270 m depth.

Pyroxene is the second most abundant primary mineral in the cuttings of the well. It appears as phenocrysts and as part of the groundmass. It forms subhedral to euhedral phenocrysts. In thin sections it is observed that, below 519 m depth, pyroxene is partially altered into clay and calcite and at 1281 m it is replaced by actinolite. Generally pyroxene is very resistant to alteration in well SJ9-2. However, at 72 m completely altered pyroxene appears.

Opaque minerals: these minerals comprise FeTi-oxides and are generally crystallised as part of the primary rock constituents; they are visible throughout the well.

4.2 Distribution of hydrothermal minerals

The alteration mineral paragenesis of well SJ9-2 is shown in Figure 7. The most common hydrothermal alteration minerals are quartz, calcite, and pyrite and low-temperature minerals such as heulandite, stilbite, laumontite and smectite. These minerals are followed by high-temperature minerals such as chlorite, illite, and epidote.

Calcite commonly replaces plagioclase with the presence or absence of other secondary minerals. Calcite formation can be linked to boiling, dilution, and condensation of carbon dioxide in the geothermal system (Simmons and Christenson, 1994). It is one of the most abundant secondary minerals.

In well SJ9-2, calcite is abundant above 1000 m depth, but decreases in some intervals such as at 700 m depth. In the bottom part of the well, calcite is sparser but never disappears which indicates that the temperature has not reached 300°C. Calcite occurs as a replacement of primary minerals or as a direct deposition mineral. It commonly fills the vesicles along with clay and it is also a common filling in veins along with quartz. From 99 to 681 m depth, it is possible to observe calcite in many of the depositional sequences (vesicles) where it is in the last order of the sequence. Generally, calcite replaces the primary minerals or another secondary mineral, for instance zeolite at 600 m.

Anhydrite was rare in SJ9-2. It was observed in thin sections at 600 and 1350 m depth. The presence of anhydrite in the system, together with quartz and wairakite, may signify boiling in the reservoir (Reyes, 2000). Anhydrite is also a common mineral in saline geothermal areas or in a sedimentary hosted geothermal system, where inflow of fluid with a saline composition commonly results in the precipitation of anhydrite.

Chalcedony is a silica polymorph that forms at temperatures 150-180°C. It occurs in the first 300 m of the well. Below 300 m depth, chalcedony is replaced by quartz. In thin section, chalcedony can be seen as an outer halo in the vesicles associated with clay.

Quartz: In well SJ9-2, quartz first appears around 129 m depth as a small crystal ($\geq 160-190^\circ\text{C}$). With increasing depth, it occurs as euhedral and anhedral crystals. Quartz often replaces other minerals, especially plagioclase or zeolite. It also occurs as vesicles fillings or as fine veins. At 900 m depth, transparent crystals of prismatic and euhedral quartz are common. In thin sections quartz is associated with epidote, calcite, wairakite and clay.

Zeolites: These are a large group of minerals that include hydrated aluminium silicates with alkali metals and alkalis, which form as the product of interaction between groundwater and bedrock during diagenesis. The group of zeolites includes heulandites, stilbite, mesolite, and chabasite and occurs at

temperatures below 100°C. High temperature zeolites constitute laumontite (120-220°C) and wairakite (200-300°C). The following zeolites that were found in the well were identified under the binocular and petrographic microscopes:

Heulandite was possibly recognized between 99 and 200 m depth, forming clusters of fine crystals with a vitreous aspect.

Stilbite was recognized in petrographic analyses at depths of 99, 201 and 270 m. It is characterised by radial and fan-like aggregates, and some of these fragments were altered to clay.

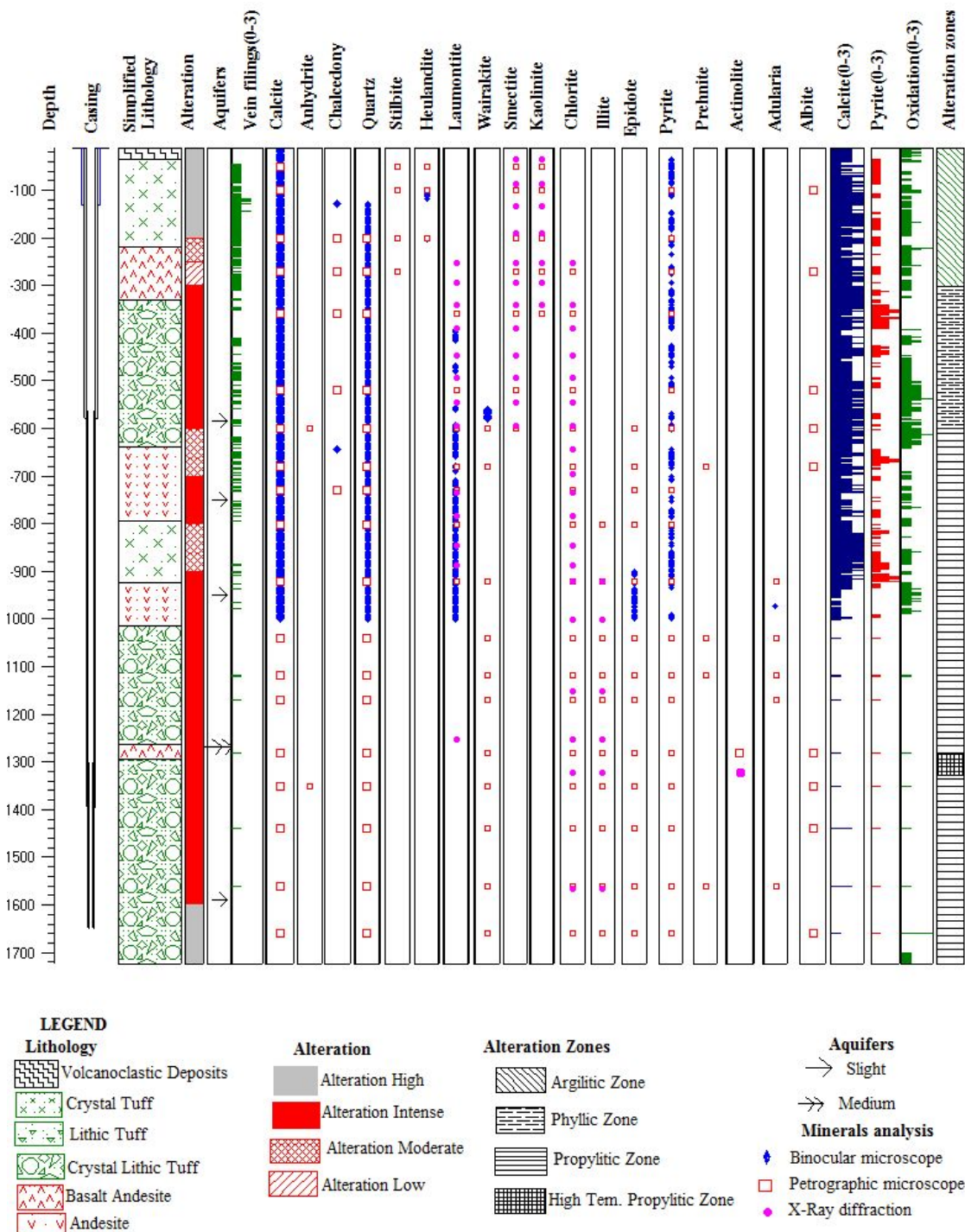


FIGURE 7: Distribution of hydrothermal alteration minerals in well SJ9-2

Laumontite: It was possible to determine this mineral in binocular and petrographic analysis. Laumontite appears at 393 m depth and disappears below 1254 m depth with a stability range in temperature from 120 and up to 190-220°C. In thin section, it was possible to observe laumontite replacing plagioclase at 519 m. It forms prismatic crystals, which are diamond-shaped and colourless.

Wairakite: This mineral appears first at 561 m depth, and is then present until the bottom of the well at 1725 m depth. Wairakite is abundant below 1000 m depth. Under petrographic microscope it is characterised by a colourless to low grey interference colour and distinct twinning.

Smectite: This type of clay is present from 12 to 645 m depth. In XRD analysis, smectite forms peaks around 12.93-13.94 Å for untreated samples, 14.1-14.67 Å for glycol treated samples and 10 Å for heated samples. In the microscope, smectite is fine-grained with a greenish-brown colour. Smectite is deposited in patches in the groundmass, fills vesicles and replaces other minerals, especially plagioclase or zeolites.

Kaolinite occurs in abundance in soils that have formed from chemical weathering of rocks in hot moist climates (Sradon, 1999) and as products of meteoric hydrothermal alteration or as rock containing feldspar and muscovite; it is also found in sediments formed by the weathering of acidic rocks. This clay appears at 36-342 m depth in the well, especially in the tuff associated with calcite and zeolites. On XRD analysis kaolinite is characterised by a peak at 7.3 Å.

Chlorite is the most extensive alteration product in well SJ9-2, appearing at 252 m depth and continues to be present along the length of the well. Petrographically, chlorite is light greenish in colour in plane polarized light and is not pleochroic. In thin sections it was possible to observe pervasive clay alteration in the samples. The chlorite alteration of plagioclase and olivine, in particular, is common as well as in the rock matrix of the tuffs. Chlorite fills vesicles and veins, often in association with smectite, in the first 594 m; below 888 m depth, it is associated with illite. In XRD analysis, chlorite is characterised by peaks at ~14.7 Å for untreated glycol treated and heated samples.

Illite appears first (along with chlorite) at 921 m depth according to XRD analyses. Illite disappears below 1152 m depth and reappears again at 1254 m depth. In XRD analysis illite is characterised by a peak at 10 Å. Petrographically, illite is colourless, forming matted flakes with a high birefringence. Illite is the product of the alteration of feldspar minerals and can be found in the groundmass, especially in tuff. Illite also occurs in altered plagioclase along with, calcite and is intergrown with chlorite at 1254 m depth.

Epidote is a light yellow - pale green mineral with a weak green colour of pleochroism. Epidote is a common mineral in geothermal reservoirs. Epidote was first identified in thin sections at 600 m depth. First epidote is very scarce, but the abundance of epidote increases below 921 m depth. Epidote is usually associated with wairakite and quartz.

Prehnite appears as a small crystal in thin sections at 681 m where it is associated with epidote. Prehnite is scarce in the entire well. Petrographically, prehnite is characterised by a high relief and strong interference colours; the typical bow-tie shape could not be clearly seen. This mineral forms at temperatures above 200-250°C.

Actinolite is a high-temperature amphibole mineral which forms when temperature has reached $\geq 280^\circ\text{C}$. In well SJ9-2 it appears in a thin section at 1281 m, replacing pyroxene and olivine. It is characterised by a fibrous shape and pleochroism. Actinolite was identified at 1323 m depth with XRD analysis; actinolite forms a peak at 8.5 Å.

Adularia was observed at 921 m in thin sections. The crystal is partly replaced by quartz and it was not possible to clearly see the characteristic diamond shape. Adularia is considered an indication of boiling of the hydrothermal fluids (Gemmell et al., 2006) and marks permeable zones (Reyes, 2000).

Albite is produced by the alteration of plagioclase. This process is known as albitization. Albite was first observed at 99 m depth and appears in many intervals along the entire well, especially where the alteration is intense at 270, 600 and 681 m.

4.3 Vesicles and veins

In the upper part of the well, vesicles in the tuffs and andesites are mostly filled with different types of clay (smectite-chlorite-illite), quartz, calcite and pyrite. However, porosity in the rock formations along the extent of the well was difficult to observe because of the small grain size of the cuttings and the high alteration of the rock.

The rock contains fine filled veins in the upper part of the well. The amount of veins decreases with depth, partly because the grain size of the cuttings becomes smaller and alteration becomes more intense, which made the veins more difficult to identify. The veins are mainly filled with calcite, quartz, pyrite and clay. Veins are most common in tuff and correlate with intervals where the tuff has a high degree of alteration, reflecting that during progressive alteration the open spaces become gradually filled with secondary minerals at their respective precipitation temperatures and fluid composition. Between 400 and 500 m depth, medium-grained veins were observed, while in the last part of the well (1000-1725 m), veins are rare and are generally filled by chlorite or calcite.

4.4 Alteration mineral zonation

Based on studies of alteration in well SJ9-2, five main zones of alteration were distinguished; each alteration zone being characterised by the dominance of particular minerals.

Argillic alteration zone (12-303 m): In this part of the well the abundance of clays is very high. This zone is represented by smectite and kaolinite in the first 300 m of the well. Kaolinite disappears at 252 m depth, while chlorite is observed first at 252 m depth. The clays are accompanied by low-temperature zeolites (heulandite, stilbite); quartz appears at 129 m. In this interval, pyrite and calcite are also present.

Phyllic alteration zone (303-519 m): This part of the well is characterised by the presence of chlorite and smectite clays. The clays are accompanied by abundant laumontite (from 393 m depth), calcite and quartz.

Propylitic alteration zone I (519-1281 m). Epidote was first identified at 600 m depth. First epidote appears in sparse amounts, but at 921 m depth epidote becomes more abundant. Epidote is accompanied by abundant laumontite between 600 and 800 m depth as well as accessory anhydrite, wairakite, adularia and prehnite. Below 921 m depth, where epidote is abundant, it is accompanied by abundant wairakite.

High-temperature propylitic zone (1281-1329 m): This zone is characterised by the appearance of actinolite in association with albite, epidote, pyrite, chlorite and quartz. The amphibole was only observed in a thin section at 1281 m depth and detected by XRD analyses at 1323 m depth.

Propylitic alteration zone II (1329-1725 m): Actinolite was not observed below 1329 m depth, while the amount of epidote increased in the formations. Therefore, the lowermost part of well SJ9-2 below 1329 m depth is characterised by propylitic alteration.

4.5 Mineral deposition sequence

The growth of new minerals from primary minerals in a rock depends on parameters such as temperature, pressure and fluid to which the rock is submitted. The environment and duration of these processes will result in the precipitation of an assemblage of stable secondary minerals. The mineral sequences deposited in vesicles and veins of well SJ9-2 were studied, based on analyses carried out with a petrographic microscope. The results are shown in Table 3.

TABLE 3: Mineral deposition sequence of well SJ9-2

Depth	Mineral Assemblages			Alteration	
	Early		Late stage		
-99	kao	still	cc	High	
-270		chl	cc	Intense	
		chl	heu MLC chal		
-360		heu	qtz lau cc	Intense	
		chal	qtz	clay	
-519	smect	chl	qtz	clay	High
		qtz	cc		
-600		lau	cc	Intense	
		cc	clay		
		qtz	cc		
		clay	qtz		
		clay	wai		
-681			epi	cc	Moderate
-729			epi	chl	Moderate
			cc	chl	
			cc	chl	
-801			chl	cc	Intense
-921			epi	ill	Intense
-1041		qtz	epi		Intense
		qtz		cc	
-1119	chl	qtz			Intense
-1170			epi	wai	Intense
			epi	qtz	
-1281			epi	qtz	Moderate
			qtz	cc	
-1350				ill	Intense
		qtz		chl	High
-1440			epi		High
-1560			epi	wai	High
			qtz	wai	

The depositional minerals were found mostly in vesicles. The mineral assemblages change with depth from low-temperature minerals such as zeolites (stilbite, heulandite) to moderate- to high-temperature minerals such as quartz, wairakite, and epidote. However, in some intervals it was not possible to see many mineral deposition sequences because of the low degree of vesicularity in the rocks and/or the high grade of alteration. Clay and calcite are the most common minerals in the mineral sequences in this well.

In the vesicles, it is possible to identify different generations of clays (chlorite, smectite, illite). For instance, it is common for clays to be the first minerals that precipitate in the vesicles, forming a thin rim or halo along the edges of the vesicles. Subsequently, quartz or calcite is precipitated in the vesicles.

The sequence generally shows that the hydrothermal system has evolved from low- to high-temperature conditions. Epidote, quartz and wairakite come later in the sequence, succeeded by chlorite or illite in the bottom part of the well. It is possible to observe calcite in many of the mineral sequences, and in the upper 700 m of the well it is commonly deposited last. Epidote is abundant below 900 m depth in SJ9-2. However, epidote is commonly not the last mineral to have formed in the mineral sequence in the lower part of the well, rather minerals such as wairakite and quartz.

5. AQUIFERS

Aquifers are typically water-saturated regions in the subsurface which produce an economically feasible quantity of water to a well. The movement of sub-surface water is controlled by the type of rock formations, the characteristics of its permeability and porosity, the temperature and pressure of the sub-surface environment, natural recharge, and the hydraulic gradient. The presence of structural formations such as faults, fractures, joints, and lithological contacts, are positive indications of geothermal feed zones (Reyes, 2000).

The formation of strong, good aquifers is very important in geothermal systems for the extraction of hydrothermal fluids and steam. The methods for determining the presence of aquifers include direct observation of circulation loss/gains during drilling, sudden changes in the rate of drilling penetration, and analysis of geophysical temperature and calliper logging. Examination of rock cuttings is an indirect approach in determining aquifers. The presence of numerous shredded rocks (mylonites), abundant vein networks, drusy and a high concentration of alteration minerals are indications of the presence of a strong sub-surface hydrological circulation. Alteration minerals such as crystallised quartz, adularia, anhydrite, wairakite, illite, hyalophane, abundant pyrite and calcite are also positive signs of good permeability. However, the absence of these alteration minerals, a low degree of alteration, the precipitation of prehnite, pumpellyite, pyrrhotite, and large quantities of laumontite and titanite can be attributed to low-permeability zones (Reyes, 2000).

Loss of circulation may vary from minor or weak loss, due to the tight characteristics of the formation, to total circulation loss that is characterised by highly permeable formations. In the geothermal system in Nicaragua, the permeable zones are associated mainly with faults and fractures in the formations (SKM, 2008a).

Well SJ9-2 was planned to intersect four permeable fault zones in the production zone (Figure 8), intercepting the NNW striking la Cholla fault, the E-W El Porvenir fault, the N-S striking SJ8 fault and the NNW striking El Tizate fault. However, the well proved to have poor permeability, achieving an injectivity of only 4 tons/hr.bar in the completion test (SKM b, 2008). The aquifers were identified according to circulation losses and temperature profiles. Six small aquifers were identified at 585, 750, 950, 1157, 1272, and 1590 m depth. The aquifers were associated with a circulation loss range of 20, 25 to 60 bbl/h. The circulation losses were very small. At 1650 m depth an attempt was made to stimulate the well by hydrofracturing with 850 bbl/h being injected under 1875 psi pressure for 61 hours. Pressure dropped 300 psi during the hydrofracturing, suggesting that the well had been slightly stimulated by this process.

The main source of permeability in the San Jacinto-Tizate field includes lithological contacts, faults and fractures. However in this study it was not possible to observe pronounced signs that the well had intersected faults. At 912 m, euhedral quartz was seen, indicating that it crystallized within larger

open spaces. Otherwise, it was not possible to observe signs of permeability along the extent of the well. This could be related to the high degree of alteration in the rock, making it difficult to observe the presence of open spaces, consistent with the poor permeability in the well.

When comparing the locations of the aquifers with the detailed geology, it is also interesting to note that some of the small aquifers could be correlated with nearby lithological contacts, such as in the interval at 1272 m depth (see Figure 7). Some relationship between the alteration minerals and permeability was, however, possible to see in the well. For instance, there was a high intensity of alteration in association with aquifers at 750 and 1272 m, and in these locations the alteration minerals were also observed to be larger (coarser), maybe due to the presence of fractures. However, at 600-800 m depth, laumontite was abundant; this is an indication of poor permeability such as in well SJ9-2.

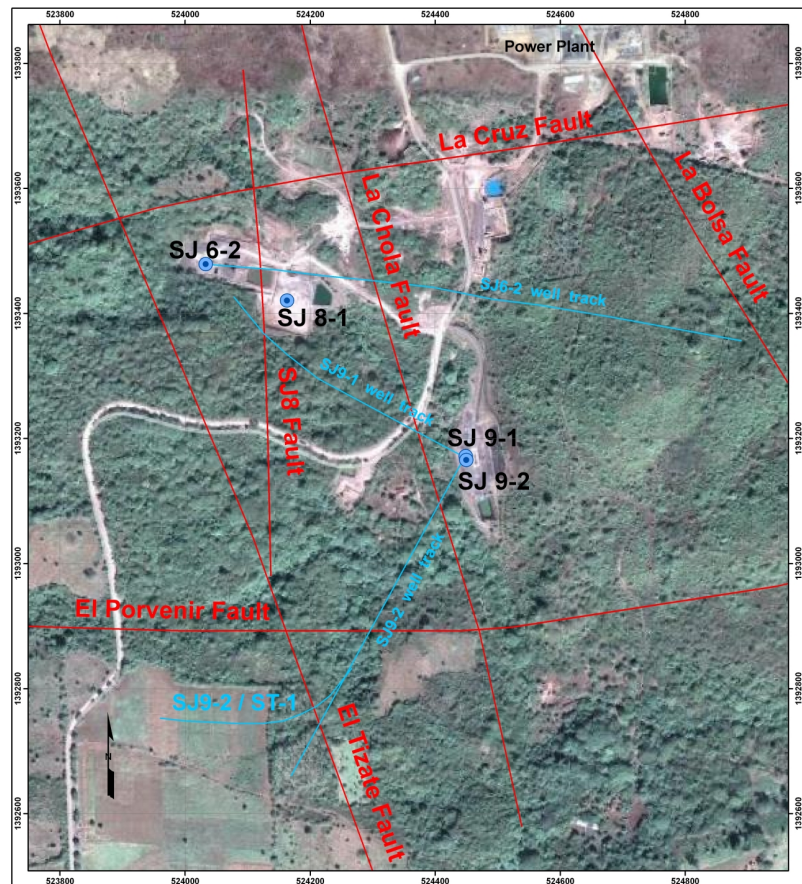


FIGURE 8: Location map showing location and actual tracks of well SJ9-2

6. FLUID INCLUSIONS AND FORMATION TEMPERATURE

Fluid inclusions in minerals represent trapped portions of liquids and gases in the crystal from which it has grown. It can be used to establish the thermal conditions in which a mineral might have formed. Inclusions formed during primary growth of a mineral are distinguished from inclusions incorporated in the host mineral during later processes after the crystal has been formed (secondary). The generally accepted mechanism for forming secondary inclusions involves the development of post crystallization fractures initiated during mechanical or thermal stress. These cracks are then sealed by later fluids to form the characteristic trails of secondary inclusions which typically crosscut earlier generations (Shepherd et al., 1985).

A total of 44 fluid inclusions in quartz crystals (it was not possible to determine the type of inclusion in the crystals) was found in well SJ9-2: five inclusions in one quartz crystal at 549-570 m and 39 inclusions in five quartz crystals at 912-921 m depth. It was not possible to find other suitable crystals, such as calcite, for the fluid inclusion studies. The fluid inclusions showed a narrow range of homogenization temperature (T_h) between 230 and 250°C (Figure 9); downhole temperatures for this well at the respective depths were measured at 220 and 250°C. The fluid inclusions were concentrated in a temperature range of 235-245°C in the first interval (549-570 m). In the second interval (912-921 m), the measured homogenisation temperature was in the range 230-250°C, but T_h values were more abundant in the interval 235-245°C indicating that the temperature had stabilized at this range. In both

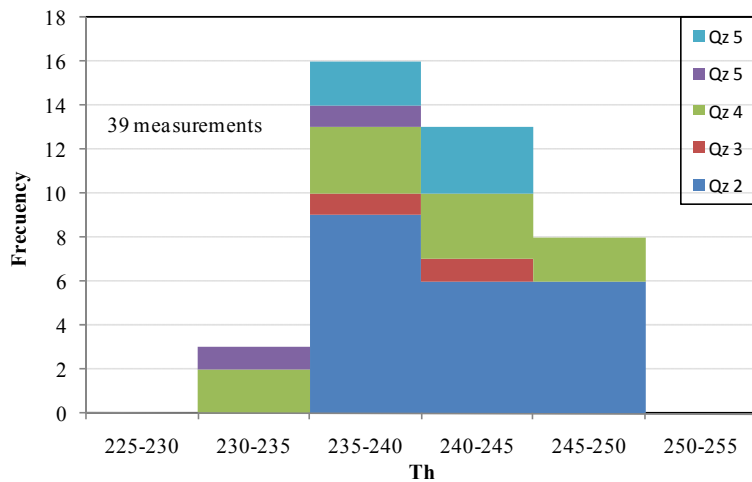


FIGURE 9: Fluid inclusions (549-570 m)

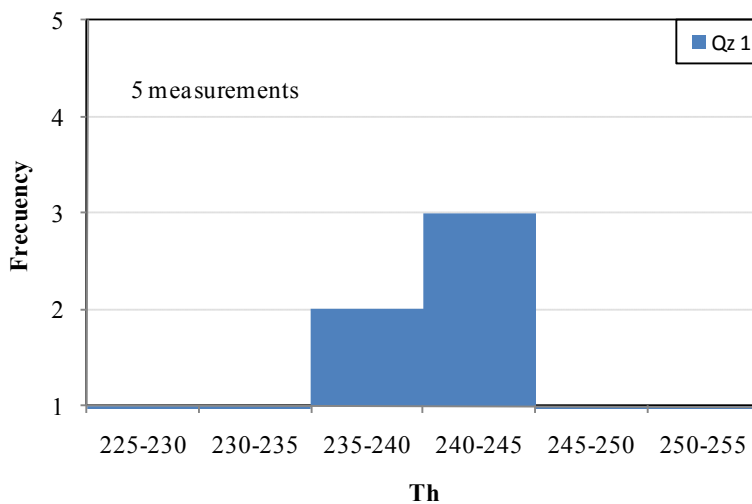


FIGURE 10: Fluid inclusions (912-921 m)

actinolite (1281 m).

Comparison of the measured homogenisation temperature in fluid inclusions with the alteration mineral temperature and the measured temperature show that the geothermal system is overall in equilibrium with a reservoir temperature of 240-255°C but, in the bottom part of the well, there is localized (30-40°C) cooling in the aquifer zone at 1250-1350 m depth.

7. DISCUSSION

Generally, the stratigraphy of well SJ9-2 consists mainly of volcanoclastic intercalations of tuff with andesite and basaltic andesite. The tuff formations have been classified into three different compositions based on their texture, crystallinity and compositional variations.

The aquifers found in well SJ9-2 are associated with lithological boundaries. Aquifers occur at different depths in the wells in the production zone, however the well was found to have poor permeability. The correlation of high alteration in the rock with the location of small aquifers is distinct. However, the presence of abundant laumontite between 600-800 m depth is associated with low permeability.

intervals, the homogenization temperature was almost the same as the formation temperature (Figures 9 and 10).

In well SJ9-2, the study of hydrothermal alteration showed the degree and intensity of rock alteration as well as the alteration mineral distribution according to the depth and temperature in the geothermal reservoir (Figure 11).

Hydrothermal alteration mineral temperature was determined according to the first appearance of selected alteration minerals (Table 1). The current formation temperature of the well (240-255°C) was determined based on the temperature measurements logged in the well during the temperature recovery period.

The alteration temperature curve showed a progressive temperature increase with depth. Low-temperature minerals such as zeolites (heulandite, stilbite) formed at shallow levels (50-200 m) (see Figure 11), followed by laumontite (393 m) and later by high-temperature minerals such as wairakite, epidote (600 m) and

Well SJ9-2 was drilled to obtain permeability through the intersection of three main vertical faults. Taking into account the low permeability in the well and its correlation with the small aquifers and the degree of alteration, it could be assumed that fractures have been sealed by mineral deposition.

The distribution of hydrothermal alteration minerals showed a progressive variation with temperature. The mineral assemblages changed from clay (smectite) and low temperature zeolites (stilbite, heulandite) at 36 m depth, followed by higher temperature minerals such as laumontite (393 m), wairakite (519 m), sparse epidote (600 m) and actinolite in the deeper parts (1281 m). Based on the formation of these progressive temperature-dependent minerals, five zones of hydrothermal alteration were identified in the studied well, each characterised by the first appearance or the dominance of the respective mineral.

These zones are: argillic zone (12-303 m), phyllic zone (303-600 m), propylitic zone I (600-1281 m), high-temperature propylitic zone (1281-1329 m), and propylitic zone II (1329-1725 m).

Comparison of the fluid inclusions, formation temperature and alteration temperature in well SJ9-2 showed that, generally, the alteration mineralogy was in accordance with the range of the formation temperature. However, cooling was observed at 1281-1329 m depth in the well. At this depth, actinolite was present at an interval where the measured temperature today is ~250°C. This is 30°C lower than the normal temperature stability range of actinolite ($\geq 280^\circ\text{C}$). The increased alteration at this depth could be associated with an aquifer in this zone which has subsequently cooled. The fluid inclusion measurements in the two intervals at 549-570 and 912-921 m depth showed a temperature range of 235-255°C. This is overall in agreement with the current temperature in the reservoir today, indicating that the change in temperature is minor in this part of the reservoir (Figure 10). The fluid inclusion measurements were based on quartz analyses. Further analyses of other alteration minerals such as calcite are required for validation.

A significant feature in the well is at the interval between 600 and 800 m depth, where there appeared to be some disequilibrium in the alteration mineral assemblage. At this interval, laumontite was

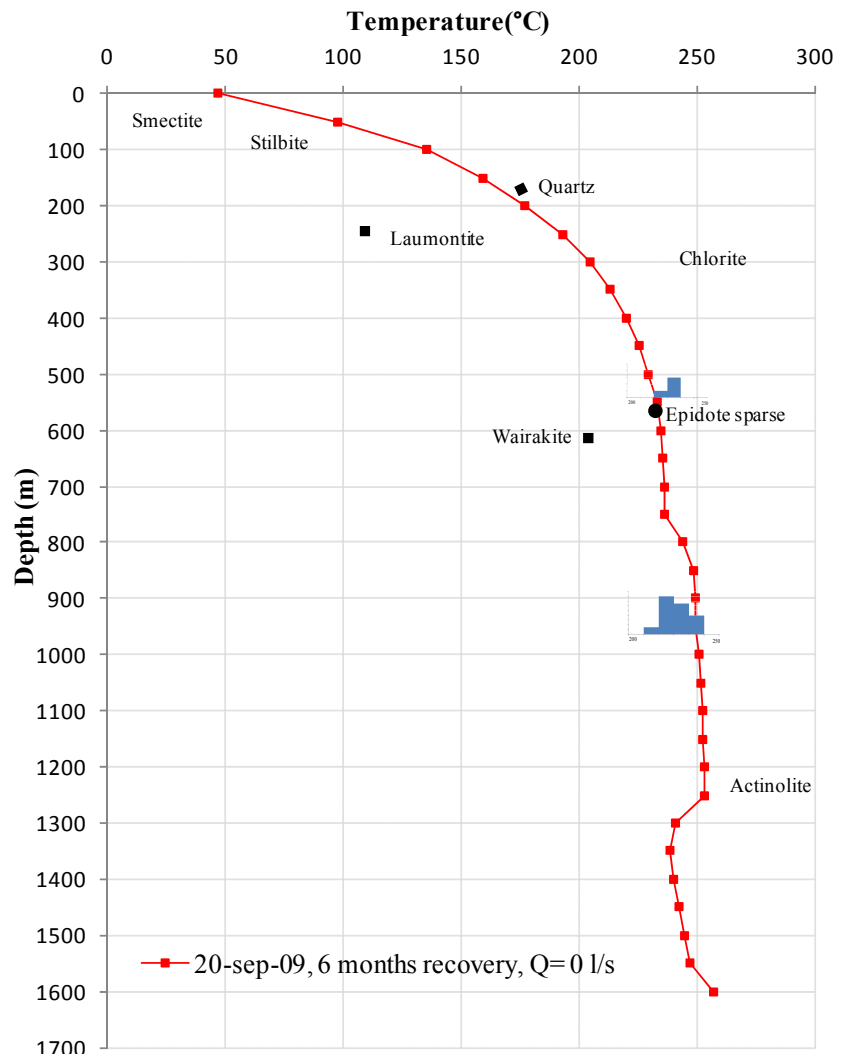


FIGURE 11: Profile of formation temperature, alteration mineral temperature and homogenization temperature in fluid inclusions at 549-570 m and 912-921 m

abundant, but laumontite is not stable at temperatures above 190-220°C. Despite the abundance of laumontite, epidote was first observed at 600 m depth. Epidote was not abundant until 921 m depth; the temperature was in the range of 230-250°C at 600-921 m depth. The coexistence of laumontite and epidote at 600-800 m depth may be due to poor permeability in the well, thus requiring more time before the alteration mineralogy can equilibrate to the new temperature conditions. Similarly, illite did not appear until 900 m depth, despite the fact that the presence of illite normally persists when temperatures have reached $\geq 230^\circ\text{C}$. It is expected that illite appears at a similar depth as epidote in geological formations of intermediate to evolved composition. The most plausible explanation for the absence of illite at 600-900 m depth would again be low permeability, lengthening the reaction time for alteration minerals, delaying equilibration at advanced temperatures.

At 1281 m depth, the presence of actinolite in a restricted zone indicated that the temperature at one time had reached more than 280°C. Correlation with the current formation temperature shows that temperature decreased 30°C at this depth. In the lower part of the well, epidote was abundant along with wairakite and quartz; the two latter minerals commonly represent the last phase of alteration mineral deposition. At shallower levels of the well, it was similarly observed that epidote was not the last phase of mineral deposition. This seems to reflect that there has been some minor fluctuation in temperature in the reservoir over time.

8. CONCLUSIONS

These conclusions can be deduced:

- The stratigraphy of well SJ9-2 consists of a volcanoclastic sequence: intercalations of tuff, andesite and basaltic andesite. Intrusive rocks are not present.
- According to the distribution of alteration minerals, five alteration zones were identified: argillic zone (12-303 m), phyllic zone (303-519 m), propylitic zone I (519-1281 m), high-temperature propylitic zone (1281-1329 m), and propylitic zone II (1329-1725 m).
- According to the hydrothermal alteration minerals, the temperature showed a progressive temperature increase with depth, first with the appearance of minerals such as low-temperature zeolites, quartz, and smectite. The alteration was high below 519 m depth with the appearance of epidote (sparse) and wairakite ($\geq 230^\circ\text{C}$). The alteration increased below 900 m depth (abundant epidote, $\geq 250^\circ\text{C}$) and localized at 1250-1350 m depth (+actinolite, $\geq 280^\circ\text{C}$).
- Comparison of alteration mineral temperature and measured temperature showed that the geothermal system is overall in equilibrium with a reservoir temperature of 240-260°C. There was localized $\sim 30^\circ\text{C}$ cooling at the aquifer zone at 1250-1350 m depth. Abundant laumontite at 600-800 m depth may be due to low permeability.
- According to circulation loss data, temperature logs and alteration, six small aquifers were identified in the production section. Permeability is low and appears to be associated with lithological contacts.

ACKNOWLEDGMENTS

I extend my sincerest gratitude to the most important person in my life, my husband Harlan Jeancarlo, for his love and support during this six months; this is for you, T.A., and my parents and sisters for their prayers which are part of me.

My gratitude is expressed to the Government of Iceland, the United Nations University Geothermal Training Programme and the Government of Nicaragua, for giving me the opportunity to participate in this training. My gratefulness goes to Dr. Ingvar B. Friðleifsson and Mr. Lúdvík S. Georgsson for their support in completing this training. I also thank very much Thórhildur Ísberg, Dorthe H. Holm and Markús A.G. Wilde for their help during these 6 months.

My special thanks go to my supervisor, Ms. Anette K. Mortensen, for her excellent guidance of this project and for providing me with knowledge for the future, and to Dr. Hjalti Franzson for his support and teaching during this training. Thanks also to Mr. Sigurður Sveinn Jónsson for his kind help in the preparation of clay samples for XRD analysis.

I would also like to thank my friends and workmates, Ms. Juanita Ruiz and Ms. Magdalena Perez, for their help and support; I extend my appreciation to my boss, Mr. Mario Gonzales, for supporting this project. Thanks to all the UNU fellows for their friendship and support.

Finally, I would like to express my gratitude to my God and the Holy Virgin for giving me this blessing.

REFERENCES

- Browne, P.R.L., 1978: Hydrothermal alteration in active geothermal fields. *Ann. Rev. Earth & Planet. Sci.*, 6, 229-250.
- CNE, 2001: *Nicaragua geothermal master plan*. National Energy Commission of Nicaragua (CNE) and GeothermEx, report, vol. X, 28 pp.
- Franzson, H., 2010: *Borehole geology*. UNU-GTP, Iceland, unpubl. lecture notes.
- Gemmell, J.B., and the AMPIRA P588 team, 2006: Exploration implications of hydrothermal alteration associated with epithermal Au-Ag deposits. *Proc. of the Australian Earth Sciences Convention 2006, Melbourne*, 5 pp.
- Henley, R.W., and Ellis, A.J., 1983: Geothermal systems ancient and modern: a geochemical review. *Earth Science and Reviews*, 19, 1-50.
- McBirney, A.R and Williams, H., 1965, Volcanic history of Nicaragua. *University of California, Geological sciences*, 55, 1-65.
- MEM, 2008: *Geological and geothermal maps of Nicaragua*. Ministry of Energy and Mines, Managua, Nicaragua, database.
- Ostapenko, S.V., Spektor, S.V., and Netesov, Y.P., 1998: San Jacinto – Tizate geothermal field Nicaragua: Exploration and conceptual model. *Geothermics*, 27, 361-378.
- Reyes, A.G., 2000: *Petrology and mineral alteration in hydrothermal systems: from diagenesis to volcanic catastrophes*. UNU-GTP, Iceland, report 18-1998, 77 pp.

Shepherd, T.J., Rankin, A.H., and Alderton, D.H.M., 1985: *A practical guide to fluid inclusion studies*. Blackie and Son, Glasgow, UK, 239 pp.

Simmons, S.F., and Christenson, B.W., 1994: Origin of calcite in a boiling geothermal system. *Am. Jour. Sci.*, 294, 361-400.

SKM, 2008a: *Drilling completion report on well SJ9-2*. Sinclair Knight Merz, unpublished report for Polaris Energy Nicaragua S.A., April.

SKM, 2008b: *Geology and petrology report on well SJ9-2*. Sinclair Knight Merz, unpublished report for Polaris Energy Nicaragua S.A., April.

Spektor, S.V., 1994: *Report on geologic map of San Jacinto - Tizate geothermal field, Nicaragua*. Intergeoterm, S.A., unpublished report, 22. Pp.

Sradon, J., 1999: Nature of mixed-layer clays and mechanisms of their formation and alteration. *Ann. Rev. Earth & Planet. Sci.*, 27, 19-53.

Weinberg, R., 1992: Neotectonic development of western Nicaragua. *Tectonics*, 11, 1010-1017.

APPENDIX I: Results of the XRD analysis of clay minerals

Depth m	d(001) UNT	d(001) GLY	d(001) HIT	d(002)	Mineral	Remarks	Other minerals
36	13,88	14,67	10		Sm:sm		7,3 Å kaolinite
87	13,94	14,39	10		Sm:sm	9,2Å?	7,3 Å kaolinite
135	13,7	14,4	10		Sm:sm	9,2Å?	7,3 Å kaolinite
192	nd	nd	nd		no clay		
252	15,1	15,1	nd		Chl.	9,7Å? (8,8Å HIT)	
295	12,93	14,1	10		Sm:sm	9,2Å?	7,3 Å kaolinite
342	14,1	14,1	14,1/10	7,25 HIT=0)	Chl.:sm.	9,7Å? (8,8Å HIT)	(kaolinite ? 7,2Å)
390	14,4	14,4	14,4/10	7,22 HIT=0)	Chl.:sm.	9,2Å?	Laumontite
447	14,4	14,4	14,4/10	7,22 HIT=0)	Chl.:sm.	9,7Å?	Laumontite
495	14,4	14,4	14,4/10	7,22 HIT=0)	Chl.:sm.	9,7Å? 9,2Å	Laumontite
546	14,7/11,2	14,7/11,2	14,7/10	7,20 HIT=0)	chl. (sm)	9,7Å? (8,8Å HIT)	Laumontite
594	14,5/10,7	14,5/10,7	14,4/10	7,20 HIT=0)	chl. (sm)	9,7Å? (8,8Å HIT)	Laumontite
645	nd	nd	nd				
696	14,8	14,8	14,8	7,2 (HIT=0)	Chl. unst		
735	14,8	14,8	14,8	7,2 (HIT=0)	Chl. unst	9,7Å? (8,8Å HIT)	Laumontite
783	14,6	14,6	14,6	7,2 (HIT 7,2 med)	Chl.	9,7Å? (8,8Å HIT)	Laumontite
846	14,6	14,6	14,6	7,2 (HIT 7,2 med)	Chl.	9,7Å? (8,8Å HIT)	Laumontite
888	14,6	14,6	14,6	7,2 (HIT 7,2 med)	Chl.	9,7Å? (8,8Å HIT)	Laumontite
921	14,6	14,6	14,6	7,2 (HIT 7,2 med)	Chl. ill.		10 Å illite.
1002	14,6	14,6	14,6	7,2 (HIT 7,2 med)	Chl.	9,2Å?	
1254	14,6	14,6	14,6	7,2 (HIT 7,2 med)	Chl. ill.	7,7Å (gypsum?)	10 Å illite.
1152	14,6	14,6	14,6	7,2 (HIT 7,2 med)	Chl.		(10 Å illite.)
1323	14,6	14,6	14,6	7,2 (HIT 7,2 med)	Chl.		8,5Å amphibol
1567	14,6	14,6	14,6	7,2 (HIT 7,2 med)	Chl. ill.		10 Å illite.

APPENDIX II: Characteristic XRD patterns for the clay minerals of well SJ9-2

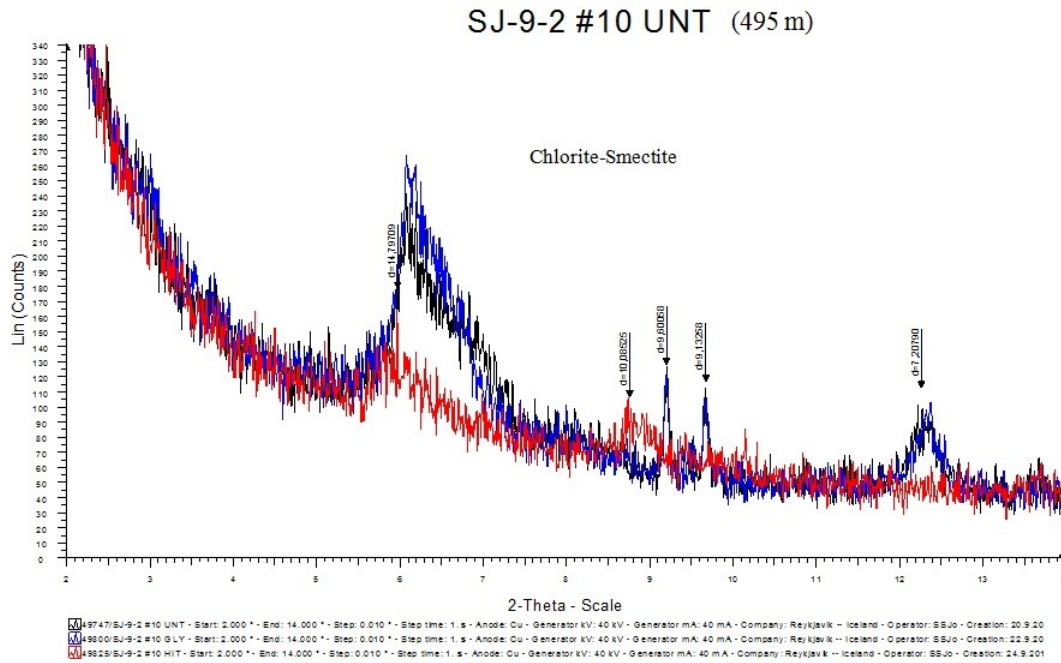


FIGURE 1: XRD analysis showing presence of chlorite and smectite

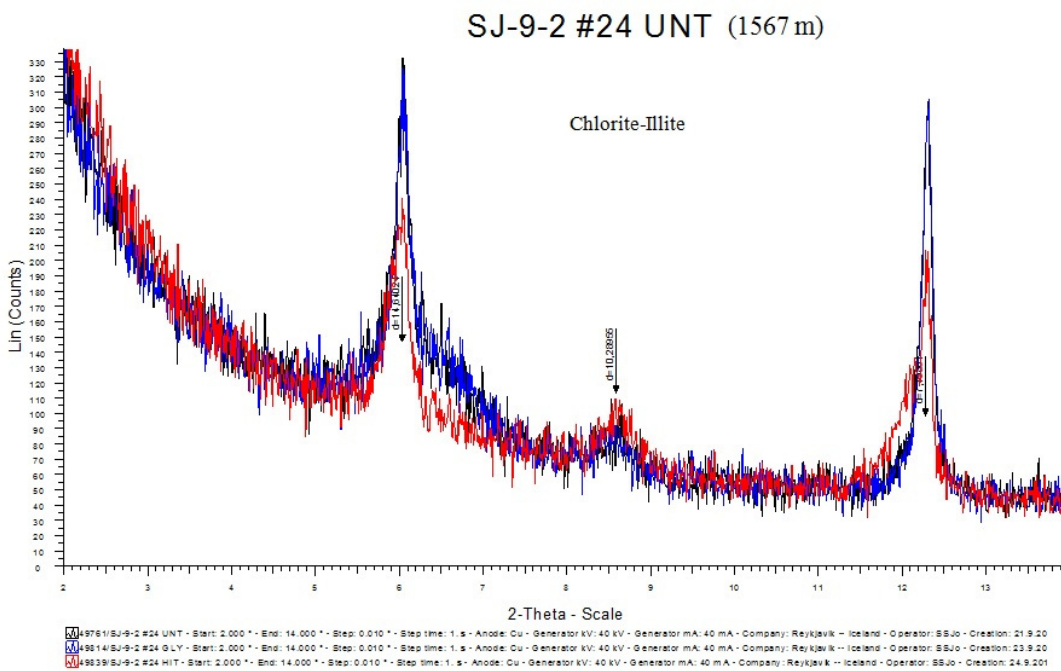


FIGURE 2: XRD analysis showing presence of chlorite and illite

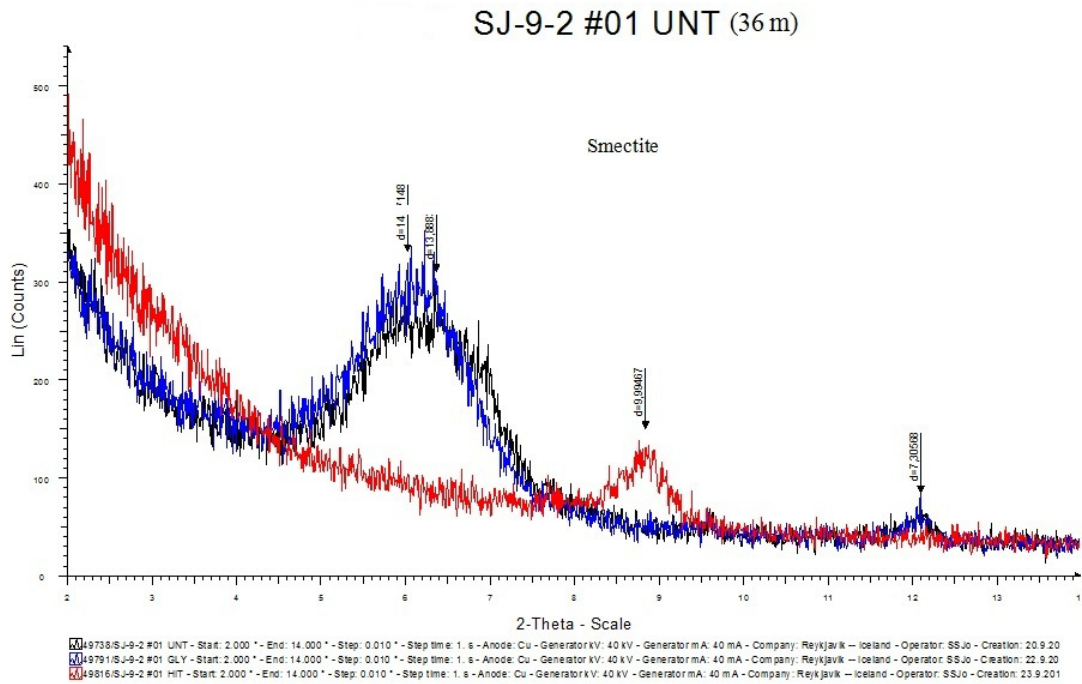


FIGURE 3: XRD analysis showing presence of smectite

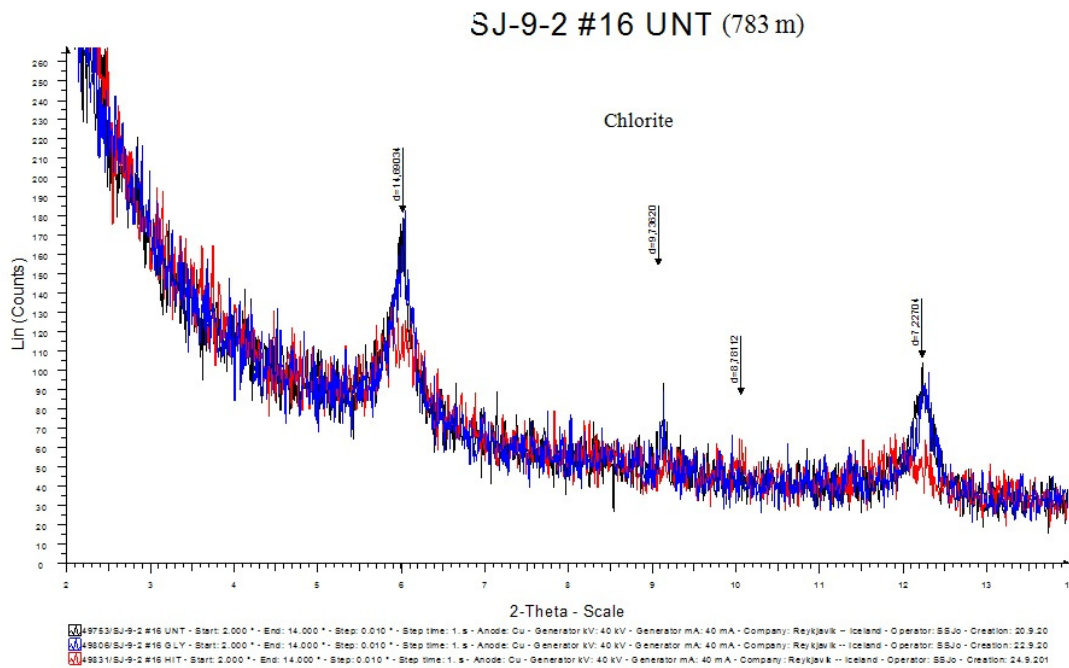


FIGURE 4: XRD analysis showing presence of chlorite